Molecular Pharmacology Fast Forward. Published on March 13, 2014 as DOI: 10.1124/mol.113.090688
This article has not been copyedited and formatted. The final version may differ from this version.

Dynamic Regulation of Rad51 by E2F1 and p53 in Prostate Cancer Cells upon Drug Induced DNA Damage under Hypoxia

Minghui Wu, Xue Wang, Natalie Mcgregor, Kenneth J Pienta, Jingsong Zhang

Department of Genitourinary Oncology and Department of Cancer Imaging and Metabolism, H. Lee Moffitt Cancer Center and Research Institute, Tampa, FL (M.W., X.W., J.Z.); University of Michigan Comprehensive Cancer Center, Ann Arbor, MI (N.M., K.J.P.)

Molecular Pharmacology Fast Forward. Published on March 13, 2014 as DOI: 10.1124/mol.113.090688
This article has not been copyedited and formatted. The final version may differ from this version.

Running title: Regulation of Rad51 upon DNA damage under hypoxia

Address correspondence to: Jingsong Zhang, H. Lee Moffitt Cancer Center and Research Institute, SRB 3, 12902 Magnolia Drive, Tampa, FL 33612
Tel: 813-745-1415; Fax: 813-745-3829; Email: jingsong.zhang@moffitt.org

Number of text pages: 32
Number of reference numbers: 35
Number of tables: 0
Number of figures: 7
Abstract word count: 228
Introduction word count: 515
Discussion word count: 1000

ABBREVIATIONS: CHIP, Chromatin immunoprecipitation; CPT-11, Camptothecin-11; Immunohistochemistry, IHC; mCRPC, metastatic castration-resistant prostate cancers; PARP, poly(ADP-ribose) polymerase; PARPi, PARP inhibitor; Homologous recombination repair, HRR.

Molecular Pharmacology Fast Forward. Published on March 13, 2014 as DOI: 10.1124/mol.113.090688
This article has not been copyedited and formatted. The final version may differ from this version.

Abstract

Intra-tumoral hypoxia has been proposed to create a "mutator" phenotype through down-regulation of DNA repair, leading to increased genomic instability and drug resistance. Such down regulation of DNA repair has been proposed to sensitize hypoxic cancer cells to DNA-damaging agents and inhibitors of DNA repair. Here, we showed that prostate cancer cells with mutant p53 were resistant to the poly(ADP-ribose) polymerase (PARP) inhibitor, veliparib and the DNA-damaging topoisomerase I inhibitor: Camptothecin-11 (CPT-11) or SN38 under hypoxia. Up-regulation of Rad51 by E2F1 upon DNA damage under hypoxia contributed to such resistance, which was reversed by either inhibiting RAD51 transcription with siRNA or by expressing wild type p53 in the p53 null prostate cancer line. Accumulation of endogenous p53, but not E2F1 and suppressed RAD51 transcription was observed in prostate cancer line with wild type p53 after DNA damage under hypoxia. Combining veliparib with CPT-11 significantly enhanced DNA damage and apoptosis under both hypoxic and normoxic culture conditions. Such enhanced DNA damage and anti-tumor activities were seen in the presence of Rad51 up-regulation and confirmed in vivo with PC3 mouse xenografts. These data illustrate a dynamic regulation of Rad51 by E2F1 and p53 in prostate cancer cells' response to hypoxia and DNA damage. The veliparib and CPT-11 combination can be further explored as a treatment for metastatic castration-resistant prostate cancers (mCRPC) that have frequent p53 mutations and enriched genomic instability.

Molecular Pharmacology Fast Forward. Published on March 13, 2014 as DOI: 10.1124/mol.113.090688
This article has not been copyedited and formatted. The final version may differ from this version.

INTRODUCTION

With the recent success of treatment of BRCA1 or BRCA2 mutated cancers with the poly(ADP-ribose) polymerase (PARP) inhibitor (Fong *et al*, 2009; Tutt *et al*, 2010) there is increasing interest to explore synthetic lethality in cancers with defective DNA repair pathways (Helleday, 2010; Yap *et al*, 2011). This could potentially offer a unique therapeutic opportunity to directly target the aggressive cancer cells that obtained genomic instability through diminished DNA repair. Although two of the most common genetic alterations in prostate cancer, ETS gene rearrangement and loss of PTEN, have been linked to sensitivity to PARP inhibition in pre-clinical studies (Brenner *et al*, 2011; Mendes-Pereira *et al*, 2009), neither of them was associated with anti-prostate cancer activities (time to disease progression, PSA response rate, or decline in circulating tumor cells) in a phase 1 study with PARP inhibitor, niraparib (Sandhu *et al*, 2013). Among the 23 prostate cancer patients in this trial, only 1 had documented BRCA mutation and 9 had stable disease for a median duration of 254 days. Developing biomarkers to identify this subgroup of prostate cancer that is sensitive to drug induced DNA damage; and improving the therapeutic index of PAPR inhibitor with novel combinations are unmet challenges.

Intra-tumoral hypoxia has been proposed to create a "mutator" phenotype with increased genomic instability and drug resistance (Bristow & Hill, 2008). This hypothesis is supported by observations that DNA repair proteins are frequently down-regulated in hypoxic cancer cells, including prostate cancer cells (Bindra & Glazer, 2007; Bindra *et al*, 2004; Chan *et al*, 2010). Down-regulation of Rad51 expression, in particular, has been reported in lung, breast, colon, prostate, and cervical cancer cell lines grown under

Molecular Pharmacology Fast Forward. Published on March 13, 2014 as DOI: 10.1124/mol.113.090688
This article has not been copyedited and formatted. The final version may differ from this version.

chronic hypoxic conditions (Bindra *et al*, 2004; Chan *et al*, 2010; Meng *et al*, 2005). Rad51 is an essential protein in homologous recombination (HRR) repair, an error-free pathway for DNA double-strand break repairs (Moynahan & Jasin, 2010). Although mutations in the RAD51 open-reading frame are rare in cancer, over-expression of Rad51 has been reported in a wide variety of cancers, especially those harboring p53 mutations (Klein, 2008). Rad51 over-expression can lead to resistance to both drug and radiation induced DNA damage and has been shown to compensate for the homologous recombination defects caused by BRCA1 or BRCA2 deficiency (Brown & Holt, 2009; Lee *et al*, 2009; Martin *et al*, 2007; Yang *et al*, 2012).

Using cell lines derived from metastatic lesions of prostate cancer patients with non-functional p53 (DU145, mutant p53; PC3, p53 null) as well as wild type p53 (LNCaP), we found that the p53 status determined prostate cancer cells' sensitivity to DNA damaging drugs under hypoxia. Prostate cancer cells with nonfunctional p53 was resistant to PARP inhibitor and topoisomerase I inhibitor under hypoxia and such resistance is mediated by up regulation of Rad51 by E2F1. The RAD51 transcription was suppressed by p53 in LNCaP cells and expressing wild type p53 in PC3 cells reversed their resistance to DNA damage under hypoxia. Combining the PARP inhibitor veliparib with CPT-11 overcame such resistance in p53 mutant prostate cancer cells and showed synergistic anti-tumor activities both *in vitro* and *in vivo*.

MATERIALS AND METHODS

Cell culture and drugs. Human prostate cancer cell lines PC3 (p53 null), DU145 (mutant p53), LNCaP (p53 wild type) and Vcap (mutant p53), were obtained from

Molecular Pharmacology Fast Forward. Published on March 13, 2014 as DOI: 10.1124/mol.113.090688
This article has not been copyedited and formatted. The final version may differ from this version.

American Type Culture Collection (ATCC, Manassas, VA, USA) and maintained in culture mediums as instructed by ATCC. For hypoxia experiments, cells were incubated in a hypoxic chamber (Biospherix, New York, NY, USA) with constant 0.2% oxygen. CPT-11/irinotecan and its active metabolite SN38 were purchased from Sigma (St. Louis, MO, USA). Unless otherwise specified in the figures, the doses of SN38 were 1 μM for PC3, 0.1 μM for DU145 and 0.5 μM for LNCaP . The PARP inhibitor veliparib/ABT888 was kindly provided by Abbott Laboratories (Abbott Park, IL, USA) and 1 μM was used in all the *in vitro* data shown in the figures.

Western blot analysis. Protein lysate preparation and immunoblotting were performed as described previously (Zhang *et al*, 2004). Antibodies to PARP, E2F1, E2F4, p53, Rad51, poly ADP Ribose(PAR), γH2AX, β-Actin, and tubulin were purchased from Cell Signaling (Boston, MA, USA), Santa Cruz biotechnology (Santa Cruz, CA, USA), Trevigen (Gaithersburg, MD, USA), Millipore (Billerica, MA, USA), and Sigma-Aldrich (St. Louis, MO, USA). Immunoreactive protein was detected using ECL reagents (Roche, Indianapolis, IN, USA) according to the manufacturer's instructions.

Flowcytometry. Cells were collected and analyzed for apoptosis with propidium iodide and annexin V (BD Biosciences, San, Jose, CA, USA). The stained cells were sorted by FACSCAN1 (BD Biosciences, San, Jose, CA, USA), and data were analyzed with Flowjo software (Tree Star Inc, Ashland, OR, USA).

Molecular Pharmacology Fast Forward. Published on March 13, 2014 as DOI: 10.1124/mol.113.090688
This article has not been copyedited and formatted. The final version may differ from this version.

Real-time reverse transcription PCR. Total RNA was extracted using RNeasy Mini kit (Valencia, CA, USA); 2 μg total RNA was reversely transcribed using SuperScript II Reverse Transcriptase (Applied Biosystems, Grand Island, NY, USA) according to the manufacturer's instructions. Sequences of RAD51 primers were as follows: GCTGCGGACCGAGTAATG (forward) and CCAGCTTCTTCCAATTTCTTC AC (reverse). Amplification reaction assays contained 1× SYBR green PCR Mastermix (Applied Biosystem, Grand, Island, NY, USA) at the optimal concentrations, and amplification was performed using an ABI PRISM 7000 SDS thermal cycler (Applied Biosystem, Grand Island, NY, USA). GADPH was used as the reference gene for normalization.

Gene silencing with siRNA. RAD51 siRNA pools (3 target specific siRNAs) were purchased from Santa Cruz Biotechnology (Santa Cruz, CA, USA). E2F1 siRNA Smartpools (4 target specific siRNAs) were purchased from Dharmacon (Pittsburgh, PA, USA). PC3 or DU145 cells were seeded in 6-well plates and transfected with 5μM siRNAs. After 6 hours, the medium with siRNA was removed and cells were incubated with fresh medium overnight before further treatment. A mock siRNA (Pittsburgh, PA, USA) was used as control.

Reporter assays. The RAD51 promoter PGL3 luciferase reporter construct and the construct with mutated E2F1 binding site at RAD51 promoter were kindly provided by Dr. Peter Glazer. Cells were seeded in 96-well culture plates and transfected with 2 ng/well Renilla luciferase construct along with 0.2 μg/well of each RAD51 promoter

Molecular Pharmacology Fast Forward. Published on March 13, 2014 as DOI: 10.1124/mol.113.090688
This article has not been copyedited and formatted. The final version may differ from this version.

firefly luciferase reporter construct in triplicate. Firefly and Renilla luciferase activities were measured with the Dual-Luciferase Reporter Assay kit (Promega, Fitchburg, WI, USA).

Chromatin immunoprecipitation (ChIP) assay. ChIP experiments were performed with the Chip-IT Express Kit (Active Motif, Carlsbad, CA, USA). Briefly, cells were cross-linked with formaldehyde and incubated with 1X lysis buffer with a protease-inhibitor mixture, and sonicated to generate 200-500bp DNA fragments. After incubation with 5 µg of anti-p53 antibody or anti-E2F1 antibody, the cross-linking was reversed. The bound DNA was obtained by phenol chloroform extraction and ethanol precipitation, and resuspended in 50µl of H_2O. PCR was performed with 5 µl of immunoprecipitated target DNA. Input material corresponding to 1% of total sample was recovered prior to inmunoprecipitation, and PCR was performed with 1 µl of purified DNA. Primer sets used were the following: 5´-CCTCGAACTCCTAGGCTCAGA-3´, 5'-CCGCGTCGACGTAACGTAT-3', for the p53 binding sites on the RAD51 promoter; and 5´-TAGGAGGCTCAGAGCGACCA-3´, 5'-GTCCGCCAGCGGCTTTCAGAA -3', for the E2F1/E2F4 binding site on the proximal RAD51 promoter.

Adenoviral Infection. Recombinant adenovirus containing wild-type p53 and green fluorescent protein (*GFP*), *p53/GFP adenovirus 5*, and the empty vector *GFP adenovirus 5* were purchased from vector biolabs (Philadelphia, PA, USA). PC3 cells were infected with 200 pfu/cell of either *GFP adenovirus 5* or *p53/GFP adenovirus 5*. Infection efficiency was monitored by observation under fluorescent microscope. The plates with sufficient infection efficiency were used (>90%).

Molecular Pharmacology Fast Forward. Published on March 13, 2014 as DOI: 10.1124/mol.113.090688
This article has not been copyedited and formatted. The final version may differ from this version.

Neutral comet assay. The neutral comet assay was used to detect DNA double-strand breaks and was carried out based on manufacturer's instructions (Trevigen, Gaithersburg, MD, USA). Comets were visualized with the Olympus BX51 fluorescence microscope.

Clonogenic assay. Cells were seeded in 6-well plates to reach 70-80% densities and cultured for at least 24 hours before treatment with SN38, veliparib, or their combination for 16 hours. Treated and untreated cells (n = 1000 each) were seeded separately in 6-well plate for 14 days to form colonies. After washing with PBS, colonies were fixed with 100% methanol, dried, stained with 0.5% crystal violet (Sigma Adrich, St. Louis, MO, USA), and counted manually.

Immunofluorescence staining and confocal microscopy. Cells were seeded onto Lab TekII chamber slides (Fisher Scientific, Hampton, New Hampshire). The immunofluorescence assay was performed as described previously (Zhang *et al*, 2004). Mouse anti-Rad51 (Abcam, Cambridge, MA, USA) and rabbit anti-BRCA1 (Santa Cruz Biotechnology, Santa Cruz, CA, USA) were used as primary antibodies. The Alexa Fluor 488 goat anti-mouse antibody (Invitrogen, Carlsbad, CA, USA) and the Alexa Fluor 594 goat anti-rabbit antibody (Invitrogen, Carlsbad, CA, USA) were used as secondary antibodies. The coverslips were mounted with DAPI containing Vectashield (Vector Laboratories, Burlingame, CA, USA). Samples were viewed with a Leica DMI6000 inverted microscope, TCS SP5 confocal scanner, and a 63X/1.4NA Plan Apochromat oil immersion objective (Leica Microsystems, Buffalo Grove, IL, USA). Images were

Molecular Pharmacology Fast Forward. Published on March 13, 2014 as DOI: 10.1124/mol.113.090688
This article has not been copyedited and formatted. The final version may differ from this version.

captured with photomultiplier detectors and prepared with the LAS AF software version 1.6.0 build 1016 (Leica Microsystems, Buffalo Grove, IL, USA).

Immunohistochemistry (IHC). IHC analyses for pimonadazole (Hydroxyprobe, Burlington, MA, USA), γ-H2AX (Millipore, MA, USA), and Rad51 (Abcam, Cambridge, MA, US) on FFPE xenograft sections were performed at Moffitt Cancer Center's Tissue Core with the standard antigen retrieval method. Consecutive xenograft sections were used to closely match the pimonadazole positivity with the γ-H2AX and Rad51 stains.

Xenograft studies. The xenograft study protocol was approved by the Institutional Animal Care and Use Committees. Xenografts were established by subcutaneous injection of 5.0×10^5 PC3 cells 1:1 mixed with matrigel (BD Bioscience, San Jose, CA, USA) to the flank area of male NOD.CB17-Prkdcsid/NcrCrl mice. After the xenografts reached ~200 mm^3, mice were randomized to treatment groups of saline control, CPT-11, veliparib, and veliparib combined with CPT-11. Male mice were weighted and xenograft size were measured twice per week. Mice were euthanized when the xenografts reached 1000 mm^3. At day 101, all of the remaining mice underwent euthanasia regardless of their xenograft size. To highlight the hypoxic regions, pimonadazole was injected before mice were euthanized. The mice received 1 day of assigned treatment prior to euthanizing if the xenografts grew to the 1000 mm^3 threshold while being off treatment. This allowed us to assess the effects of treatment on DNA damage and DNA repair with these xenograft samples.

Molecular Pharmacology Fast Forward. Published on March 13, 2014 as DOI: 10.1124/mol.113.090688
This article has not been copyedited and formatted. The final version may differ from this version.

Statistical analysis. Statistical analysis was performed using the GraphPad Prism 5 software. For one-way ANOVA, Tukey's multiple comparison test was used. T-test was used for two-group comparisons. Data derived from at least 3 independent experiments were shown as means ± SEM. Log-rank test was used for survival rate analysis in the mouse xenograft experiments. $*P < 0.05$, $**P < 0.01$, $***P < 0.001$.

RESULTS

Up regulation of Rad51 contributes to prostate cancer cells' resistance to drug induced DNA damage under hypoxia. Unlike LNCaP cells (wild type p53), PC3, Vcap and DU145 cells (p53 null or mutant) continue to proliferate under chronic hypoxia (0.2% oxygen) (Figure 1A). Although Rad51 was initially decreased under hypoxia, up regulation of Rad51 was observed in PC3 and DU145 cells after 3-day treatment with Topoisomerase I inhibitor, SN38 (Figure 1B). Compared to PC3 and DU145 cells treated with SN38 under normoxia, the up regulations of Rad51 after SN38 treatment under hypoxia were associated with less DNA double-strand breaks as detected by γH2AX levels on western blot (Figure 1B); and less apoptosis as measured by PARP cleavage on western blot (Figure 1B) and propidium iodide-annexin V-positive cells on flowcytometry (Figure 1C). No up regulation of Rad51 was observed in LNCaP after treatment with SN38 under hypoxia. Compared to LNCaP cells grew under normoxia, LNCaP cells grew under hypoxia remained sensitive to SN38 induced DNA damage and apoptosis (Figure 1, B and C).

Formations of Rad51 and BRCA1 nuclear foci on immunofluorescence were used to reflect the activation of the homologous recombination repair (Scully *et al*, 1997).

Molecular Pharmacology Fast Forward. Published on March 13, 2014 as DOI: 10.1124/mol.113.090688
This article has not been copyedited and formatted. The final version may differ from this version.

Compared to untreated PC3 cells under normoxia, there was less nuclear staining of Rad51 and BRCA1 under hypoxia (Figure 2A). This is consistent with less DNA damage caused by oxidative stress (Figure 1B) and therefore less demand for DNA repair proteins like Rad51 and BRCA1 under hypoxia. No changes in the levels of key proteins in the non-homologous end joining pathway were observed when SN38-treated cells were compared to untreated cells under either normoxia or hypoxia (Figure 2B).

Whether blocking Rad51 expression could re-sensitize mCRPC cells to the topoisomerase I inhibitor under hypoxia was then studied. As shown in Figure 2C, Rad51 protein levels can be effectively decreased with siRNA. Compared to untreated PC3 cells under hypoxia, higher levels of Rad51 were observed after SN38 treatment in untransfected and mock siRNA transfected PC3 cells, but not RAD51 siRNA transfected PC3 cells. DNA damage/γH2AX levels (Figure 2C) and apoptosis (Figure 2D) after SN38 treatment under hypoxia were significantly increased after blocking Rad51 up-regulation with siRNA. These data indicate that prostate cancer cells' resistance to drug induced DNA damage under hypoxia requires up regulation of Rad51 and Rad51 mediated DNA repair.

PARP inhibitor, veliparib overcomes p53 mutant prostate cancer cells' resistance to topoisomerase I inhibitor under hypoxia and enhances its anti-tumor activities.

Accumulating data supports the synergies between PARP inhibitor and topoisomerase I inhibitor under normoxia (Patel *et al*, 2012; Smith *et al*, 2005; Zhang *et al*, 2011). We therefore tested whether adding veliparib can re-sensitize p53 mutant prostate cancer cells to SN38 under hypoxia. As shown by the diminished PAR level, 1 uM of veliparib

Molecular Pharmacology Fast Forward. Published on March 13, 2014 as DOI: 10.1124/mol.113.090688
This article has not been copyedited and formatted. The final version may differ from this version.

was sufficient to inhibit PARP activity under hypoxia (Figure 3A). When DNA damage was assessed by γH2AX levels in Western blot and tail moment in neutral comet assay, veliparib as a single agent caused minimum DNA damage. Combining veliparib with SN38 significantly enhanced the DNA damage induced by SN38 under the hypoxia (Figure 3, A and B).

The anti-tumor activities of veliparib, SN38 and their combination were then assessed *in vitro* and *in vivo*. Although veliparib had no single agent anti-tumor activities, its combination with SN38 significantly enhanced apoptosis (Figure 3C) and decreased colony formation (Figure 3D) in PC3 and DU145 cells compared to those treated with single agent SN38. Compared with untreated cells, a dose-dependent decrease in colony formation after SN38 treatment was also observed (Figure 3D). Based on published xenograft studies with CPT-11, we initially used 60 mg/kg intraperitoneal injection on day 1 and day 5 of every 21 days cycle. Although adding veliparib oral gavages at 12.5 mg/kg on weekdays to CPT-11 led to decreased tumor volume (Figure 4A), this schedule (*schedule A*) was not well tolerated. Two of the 8 mice in the combination treatment group were excluded in the analysis due to early death at day 35 (day 14 of cycle 2). We then modified the schedule (*schedule B*) based on the phase I study combining veliparib with CPT-11 in non-prostate tumors reported at the American Society of Clinical Oncology (ASCO) 2011 annual meeting (abstract 3000). In Figure 4B, CPT-11 was given at day 1 and day 8 of every 21-day cycle. Two veliparib schedules were tested: twice daily (V_{21} in Figure 4) and twice daily for 14 days of each 21 day cycle (V_{14} in Figure 4). Compared to the growth curves and survival curves of saline control, single agent CPT-11 significantly inhibited the growth of PC3 xenografts (Figure 4B) and prolonged

Molecular Pharmacology Fast Forward. Published on March 13, 2014 as DOI: 10.1124/mol.113.090688
This article has not been copyedited and formatted. The final version may differ from this version.

survival of the mice (Figure 4C). Consistent with the *in vitro* data, veliparib had minimal single agent activities on the doses and schedules tested. Adding valiparib to CPT-11 significantly enhanced the growth inhibition and survival benefit of CPT-11 (Figure 4, B and C).

The expression of markers for intra-tumor hypoxia (pimonadazole), DNA damage (γH2AX), and repair (Rad51) were then studied with IHC on the PC3 xenograft sections. As shown by the IHC image of γH2AX positivity and intensity, adding veliparib enhanced the DNA damage caused by CPT-11 (Figure 4D). Most of the DNA damage/ γH2AX staining in the CPT-11 treated xenograft were in the normoxic/ pimonadazole negative area; whereas DNA damage/γH2AX staining were seen in both the hypoxic/pimonadole positive and normoxic/pimonadazole negative areas in the valiparib and CPT-11 treatment group (Figure 4D, panel C vs. V_{14}+C). Moreover, positive Rad51 staining was noted in both the hypoxic and normoxic regions in the valiparib and CPT-11 treatment group (Figure 4E). This is consistent with our *in vitro* finding that adding veliparib overcomes p53 mutant prostate cancer cells' resistance to topoisomerase I inhibitor under hypoxia in the presence of elevated Rad51.

Transcriptional regulation of Rad51 by E2F1 upon DNA damage under hypoxia.

Among the E2F family of transcription factors, E2F4 has been shown to suppress the transcription of RAD51 under hypoxia by binding to the E2F4 site in the proximal promoter of the RAD51 gene (Bindra & Glazer, 2007). Given that E2F1 shares a consensus binding sequence with E2F4 and both E2F1 and E2F4 can bind to the RAD51 promoter (Kachhap *et al*, 2010); the role of E2F1 in regulating Rad51 expression under

hypoxia was then studied. Compared to untreated cells under hypoxia, more than 8 folds up-regulation of RAD51 RNAs were observed after 16-hour-treatment with SN38 under hypoxia (Figure 5A, SNH vs. CH). The increase of Rad51 after treatments with SN38 and SN38 plus veliparib was associated with elevated levels of E2F1 (Figure 5B). Consistent with reduced RAD51 mRNA and protein under hypoxia, RAD51 promoter activity was significantly suppressed in untreated PC3 cells under hypoxia (Figure 5C); This promoter activity increased more than 3 folds after treating hypoxic PC3 cells with SN38 or veliparib plus SN38 (SNH and V/SH vs. CH in Figure 5C). Such increase in RAD51 promoter activity was blocked when the E2F1 and E2F4 consensus binding site on the RAD51 promoter was mutated (Figure 5C, M-SNH vs. SNH and M-V/SH vs. V/SH). Consistent with E2F4's role in down regulating RAD51 promoter (Bindra & Glazer, 2007), mutating the E2F1 and E2F4 consensus binding site led to increased RAD51 promoter activity in untreated PC3 cells under hypoxia (Figure 5C, M-H vs. CH). Of note, veliparib treatment also increased RAD51 promoter activity and protein under hypoxia and such increase was blocked after E2F binding site was mutated.

E2F1 siRNA was then used to study the regulation of Rad51 by E2F1 in PC3 and DU145 cells under hypoxia. Compared to untransfected or mock siRNA transfected cells, E2F1 protein was significantly reduced by siRNA against E2F1 (Figure 5D). Transfection with siRNA against E2F1 blocked the up-regulation of RAD51 promoter activity (Figure 5E) and Rad51 protein (Figure 5D) upon treatment of hypoxic cells with SN38, veliparib or their combination. To study the role of endogenous E2F1 in regulating Rad51, ChIP assay was performed with anti-E2F1 pull down after PC3 cells were treated with SN38 under hypoxia. Compared to untreated cells under hypoxia,

Molecular Pharmacology Fast Forward. Published on March 13, 2014 as DOI: 10.1124/mol.113.090688
This article has not been copyedited and formatted. The final version may differ from this version.

enhanced E2F1 binding to the RAD51 promoter was detected after SN38 treatment (Figure 5F). These data support the role of E2F1 in transactivating the RAD51 promoter upon drug induced DNA damage under hypoxia.

Wild Type p53 Suppressed RAD51 Transcription and Sensitize Prostate Cancer Cells to Drug Induced DNA Damage under Hypoxia. Unlike p53 null PC3 and p53 mutant DU145 cells, p53 wild type LNCaP cells were sensitive to SN38 induced DNA damage and apoptosis (Figure 1). Similar to the result observed in LNCaP, lack of Rad51 up regulations after SN38 treatment under hypoxia was observed in other cell lines with wild type p53 (A549, HCT116, and MCF7) (data not shown).

To delineate the roles of endogenous p53 and E2F1 in regulating Rad51 expression, expressions of E2F1, Rad51, p53 and its downstream effector p21 were compared at different time points after SN38 treatment in LNCaP cells under hypoxia. Increasing levels of wild type p53 and its downstream effector p21 were associated with decreasing Rad51 levels, whereas no significant changes in E2F1 levels were observed (Figure 6A). Wild type p53 was then ectopically expressed in the p53 null PC3 cells. Compared to untransfected or vector transfected PC3 cells, restoration of p53 expression suppressed the up regulation of Rad51 and increased DNA damage after SN38 treatment under hypoxia (Figure 6B).

Reporter assay and ChIP assay was then performed to study the regulation of RAD51 by p53 under hypoxia. Consistent with the decreasing Rad51 protein observed in Figure 6A, RAD51 promoter activity was suppressed after SN38 treatment compared to untreated hypoxic LNCaP cells (Figure 6C). When the occupancy of RAD51 promoter by

Molecular Pharmacology Fast Forward. Published on March 13, 2014 as DOI: 10.1124/mol.113.090688
This article has not been copyedited and formatted. The final version may differ from this version.

E2F1 and p53 were studied with the ChIP assays in hypoxic LNCaP cells, increased binding of RAD51 promoter by p53, but not E2F1 was observed after SN38 treatment (Figure 6D). These data indicate that wild type p53 plays a dominant negative role in regulating RAD51 transcription in response to drug induced DNA damage under hypoxia.

DISCUSSION

Despite recent advances in androgen deprivation therapy, immunotherapy, radiopharmaceuticals and chemotherapy, mCRPC remains an incurable disease (Liu & Zhang, 2013). Several mechanisms of therapy resistance have been studied (Seruga *et al*, 2011), and intra-tumoral hypoxia has been proposed to create a "mutator" phenotype with increased genomic instability and drug resistance (Bristow & Hill, 2008). Studies with p53 wild type lung (A549, H460), breast (MCF7), and colorectal (HCT116, RKO) cell lines have shown that down regulation of DNA repair proteins under hypoxia sensitize these cells to the PARP inhibitor and DNA damaging agents (Chan *et al*, 2010). Here we showed that prostate cancer cells with nonfunctional p53 were resistant to veliparib and the topoisomerase I inhibitor under hypoxia through transactivating Rad51 expression by E2F1. Our data support hypoxia contributes to drug resistance and such resistance in p53 mutant cells is not due to diminished, but rather more effective DNA repair when there is lack of Rad51 suppression by p53 and lack of additional DNA damage from reactive oxygen species generated under normoxia. Our preliminary data with molecular karyotyping also showed that 3 weeks of hypoxia culture and veliparib treatment did not enhance genomic instability of PC3 or DU145 cells compared to their untreated

Molecular Pharmacology Fast Forward. Published on March 13, 2014 as DOI: 10.1124/mol.113.090688
This article has not been copyedited and formatted. The final version may differ from this version.

counterparts grew under normoxia (J Zhang, unpublished data). This lack of additional chromosomal copy number changes under hypoxia and PARP inhibitor treatment is at least partly due to the preservation of DNA damage repair response in these p53 mutant cells. Our data therefore provide a mechanism other than genomic instability to explain p53 mutant cancer cells' resistance to drug induced DNA damage under hypoxia.

As shown in our proposed model (Figure 7), there is a dynamic regulation of RAD51 promoter activity by p53 and E2F1 after drug induced double strand DNA breaks. In p53 wild type prostate cancer cells, both E2F1 and p53 can bind to the RAD51 promoter under hypoxia. Upon drug induced DNA damage, increased binding of endogenous p53 to the RAD51 promoter abolished the positive regulation of RAD51 by E2F1. Without Rad51, cells cannot execute homologous recombination repair and will die from unrepaired DNA damage. In p53 mutant prostate cancer cells, enhanced binding of E2F1 to the RAD51 promoter facilitated Rad51 mediated homologous recombination repair and led to drug resistance. Of note, Rad51 over expression was frequently observed in cancers harboring mutant p53 (Klein, 2008). The suppression of RAD51 transcription by p53 provides a likely explanation.

Adding veliparib to SN-38 or CPT-11 reversed p53 mutant prostate cancer cells' resistance to DNA damage and led to cell death *in vitro* and inhibition of xenograft growth *in vivo*. Veliparib has been shown to sensitize human colon cancer, lung cancer, and glioma cells, as well as B16F10 melanoma and MX-1 breast cancer xenografts to topoisomerase I inhibitors (Patel *et al*, 2012; Smith *et al*, 2005; Zhang *et al*, 2011). Enhanced DNA damage and anti-tumor activities were also reported in phase I studies with the veliaprib -topotecan combination (Kummar *et al*, 2011) and the veliparib-

Molecular Pharmacology Fast Forward. Published on March 13, 2014 as DOI: 10.1124/mol.113.090688
This article has not been copyedited and formatted. The final version may differ from this version.

irrinotecan combination (ASCO 2011 Annual Meeting, abstract 3000). Of note, neither phase I studies included prostate cancer patients. To the best of our knowledge, our study is the first to report such activities under hypoxic condition. Several studies have explored the mechanisms underlying the synergies between the PARP inhibitor and topoisomerase I inhibitors. Using a panel of DNA repair-deficient Chinese hamster ovary cells, Smith et al. reported that the PARP inhibitor AG14361 significantly potentiated CPT-mediated cytotoxicity in all cells except in the base excision repair-deficient EM9 cells (Smith *et al*, 2005). PARP-1-dependent base excision repair was thought to be involved in the repair of DNA damage caused by topoisomerase I inhibitor. In contrast, Patel et al. recently reported that transfecting catalytically inactive PARP-1 (E988K) or transfecting the PARP-1 DNA binding domain alone to $PARP1^{-/-}$ mouse embryonic fibroblasts sensitized cells to topoisomerase I inhibitor, with cells not further sensitized by veliparib (Patel *et al*, 2012). PARP inhibition was therefore proposed to convert PARP-1 into a protein that binds to topoisomerase I-induced DNA damage, preventing its normal repair. This model of PARP inhibitor induced trapping of PARP at damaged DNA was also supported by 2 other recent publications (Murai *et al*, 2013; Murai *et al*, 2012). Given that Rad51 remained elevated in PC3, DU145 cells and PC3 xenografts treated with veliparib and topoisomerase I inhibitor, failure to release PARP after PARP inhibition can block the access of Rad51 to damaged DNA and is the likely explanation for the enhanced DNA damage observed in p53 mutant prostate cancer cells with this combination (Figure 7).

As a key DNA damage checkpoint gene, loss of functional p53 is relatively common in both primary and metastatic prostate cancer (Barbieri *et al*, 2012; Grasso *et*

Molecular Pharmacology Fast Forward. Published on March 13, 2014 as DOI: 10.1124/mol.113.090688
This article has not been copyedited and formatted. The final version may differ from this version.

al, 2012). The exome sequencing data reported by Grasso et al reported 2 point mutations and 2 frame shift mutations in 11 treatment naïve high grade primary prostate cancers (36% mutation frequency); 14 point mutations and 5 frame shift mutations in 50 heavily treated lethal castration resistant prostate cancers (38% mutation frequency). Copy number loss of p53 was also observed in 9 of these 50 lethal cases (Grasso *et al*, 2012). Prostate cancer cells with mutant p53 can therefore not only evade apoptosis, but will likely have more effective HR repair due to lack of suppression of RAD51 transcription by wild type p53. Although none of the DNA damaging chemotherapy agents has been approved for the treatment of prostate cancer, a platinum based chemotherapy regimen demonstrated a 16 months median overall survival in a phase 2 study of 120 patients who met the pre-defined criteria of anaplastic prostate cancers (Aparicio *et al*, 2013). Anaplastic prostate cancer shares several features of small cell prostate cancer and is likely enriched with cell cycle check point alterations based on its rapid proliferation. Our data highlighted the importance of p53 in determining prostate cancer cells' sensitivity to DNA damage and provide the pre-clinical rationale for testing the PARP inhibitor-irrinotecan combination in selected prostate cancer patients with mutant p53 and anaplastic feature.

Molecular Pharmacology Fast Forward. Published on March 13, 2014 as DOI: 10.1124/mol.113.090688
This article has not been copyedited and formatted. The final version may differ from this version.

ACKNOWLEDGMENTS

We thank Abbott Laboratories for providing veliparib (ABT888) and Dr. Peter Glazer at Yale University for providing the RAD51 promoter PGL3 luciferase reporter constructs.

Molecular Pharmacology Fast Forward. Published on March 13, 2014 as DOI: 10.1124/mol.113.090688
This article has not been copyedited and formatted. The final version may differ from this version.

AUTHORSHIP CONTRIBUTION

Participated in research design: Zhang, Wu, Pienta

Conducted experiments: Wu, Wang, Mcgregor

Performed data analysis: Wu, Zhang

Wrote or contributed to the writing of the manuscript: Zhang, Wu

Molecular Pharmacology Fast Forward. Published on March 13, 2014 as DOI: 10.1124/mol.113.090688
This article has not been copyedited and formatted. The final version may differ from this version.

REFERENCES

Aparicio AM, Harzstark AL, Corn PG, Wen S, Araujo JC, Tu SM, Pagliaro LC, Kim J, Millikan RE, Ryan C, Tannir NM, Zurita AJ, Mathew P, Arap W, Troncoso P, Thall PF, Logothetis CJ (2013) Platinum-based chemotherapy for variant castrate-resistant prostate cancer. *Clinical cancer research : an official journal of the American Association for Cancer Research* **19**(13)**:** 3621-3630

Barbieri CE, Baca SC, Lawrence MS, Demichelis F, Blattner M, Theurillat JP, White TA, Stojanov P, Van Allen E, Stransky N, Nickerson E, Chae SS, Boysen G, Auclair D, Onofrio RC, Park K, Kitabayashi N, MacDonald TY, Sheikh K, Vuong T, Guiducci C, Cibulskis K, Sivachenko A, Carter SL, Saksena G, Voet D, Hussain WM, Ramos AH, Winckler W, Redman MC, Ardlie K, Tewari AK, Mosquera JM, Rupp N, Wild PJ, Moch H, Morrissey C, Nelson PS, Kantoff PW, Gabriel SB, Golub TR, Meyerson M, Lander ES, Getz G, Rubin MA, Garraway LA (2012) Exome sequencing identifies recurrent SPOP, FOXA1 and MED12 mutations in prostate cancer. *Nature genetics* **44**(6)**:** 685-689

Bindra RS, Glazer PM (2007) Repression of RAD51 gene expression by E2F4/p130 complexes in hypoxia. *Oncogene* **26**(14)**:** 2048-2057

Bindra RS, Schaffer PJ, Meng A, Woo J, Maseide K, Roth ME, Lizardi P, Hedley DW, Bristow RG, Glazer PM (2004) Down-regulation of Rad51 and decreased homologous recombination in hypoxic cancer cells. *Molecular and cellular biology* **24**(19)**:** 8504-8018

Brenner JC, Ateeq B, Li Y, Yocum AK, Cao Q, Asangani IA, Patel S, Wang X, Liang H, Yu J, Palanisamy N, Siddiqui J, Yan W, Cao X, Mehra R, Sabolch A, Basrur V, Lonigro RJ, Yang J, Tomlins SA, Maher CA, Elenitoba-Johnson KS, Hussain M, Navone NM, Pienta KJ, Varambally S, Feng FY, Chinnaiyan AM (2011) Mechanistic rationale for inhibition of poly(ADP-ribose) polymerase in ETS gene fusion-positive prostate cancer. *Cancer cell* **19**(5)**:** 664-678

Bristow RG, Hill RP (2008) Hypoxia and metabolism. Hypoxia, DNA repair and genetic instability. *Nature reviews Cancer* **8**(3)**:** 180-192

Brown ET, Holt JT (2009) Rad51 overexpression rescues radiation resistance in BRCA2-defective cancer cells. *Molecular carcinogenesis* **48**(2)**:** 105-109

Chan N, Pires IM, Bencokova Z, Coackley C, Luoto KR, Bhogal N, Lakshman M, Gottipati P, Oliver FJ, Helleday T, Hammond EM, Bristow RG (2010) Contextual synthetic lethality of cancer cell kill based on the tumor microenvironment. *Cancer research* **70**(20)**:** 8045-8054

Fong PC, Boss DS, Yap TA, Tutt A, Wu P, Mergui-Roelvink M, Mortimer P, Swaisland H, Lau A, O'Connor MJ, Ashworth A, Carmichael J, Kaye SB, Schellens JH, de Bono JS

(2009) Inhibition of poly(ADP-ribose) polymerase in tumors from BRCA mutation carriers. *The New England journal of medicine* **361**(2)**:** 123-134

Fong V, Osterbur M, Capella C, Kim YE, Hine C, Gorbunova V, Seluanov A, Dewhurst S (2011) Adenoviral vector driven by a minimal Rad51 promoter is selective for p53-deficient tumor cells. *PloS one* **6**(12)**:** e28714

Grasso CS, Wu YM, Robinson DR, Cao X, Dhanasekaran SM, Khan AP, Quist MJ, Jing X, Lonigro RJ, Brenner JC, Asangani IA, Ateeq B, Chun SY, Siddiqui J, Sam L, Anstett M, Mehra R, Prensner JR, Palanisamy N, Ryslik GA, Vandin F, Raphael BJ, Kunju LP, Rhodes DR, Pienta KJ, Chinnaiyan AM, Tomlins SA (2012) The mutational landscape of lethal castration-resistant prostate cancer. *Nature* **487**(7406)**:** 239-243

Helleday T (2010) Homologous recombination in cancer development, treatment and development of drug resistance. *Carcinogenesis* **31**(6)**:** 955-960

Kachhap SK, Rosmus N, Collis SJ, Kortenhorst MS, Wissing MD, Hedayati M, Shabbeer S, Mendonca J, Deangelis J, Marchionni L, Lin J, Hoti N, Nortier JW, DeWeese TL, Hammers H, Carducci MA (2010) Downregulation of homologous recombination DNA repair genes by HDAC inhibition in prostate cancer is mediated through the E2F1 transcription factor. *PloS one* **5**(6)**:** e11208

Klein HL (2008) The consequences of Rad51 overexpression for normal and tumor cells. *DNA repair* **7**(5)**:** 686-693

Kummar S, Chen A, Ji J, Zhang Y, Reid JM, et al. Phase I study of PARP inhibitor ABT-888 in combination with topotecan in adults with refractory solid tumors and lymphomas. Cancer Res 2011; 71: 5626-5634.

Lee SA, Roques C, Magwood AC, Masson JY, Baker MD (2009) Recovery of deficient homologous recombination in Brca2-depleted mouse cells by wild-type Rad51 expression. *DNA repair* **8**(2)**:** 170-181

Liu JJ, Zhang J (2013) Sequencing systemic therapies in metastatic castration-resistant prostate cancer. *Cancer control : journal of the Moffitt Cancer Center* **20**(3)**:** 181-187

Martin RW, Orelli BJ, Yamazoe M, Minn AJ, Takeda S, Bishop DK (2007) RAD51 up-regulation bypasses BRCA1 function and is a common feature of BRCA1-deficient breast tumors. *Cancer research* **67**(20)**:** 9658-9665

Mendes-Pereira AM, Martin SA, Brough R, McCarthy A, Taylor JR, Kim JS, Waldman T, Lord CJ, Ashworth A (2009) Synthetic lethal targeting of PTEN mutant cells with PARP inhibitors. *EMBO molecular medicine* **1**(6-7)**:** 315-322

Meng AX, Jalali F, Cuddihy A, Chan N, Bindra RS, Glazer PM, Bristow RG (2005) Hypoxia down-regulates DNA double strand break repair gene expression in prostate

cancer cells. *Radiotherapy and oncology : journal of the European Society for Therapeutic Radiology and Oncology* **76**(2)**:** 168-176

Moynahan ME, Jasin M (2010) Mitotic homologous recombination maintains genomic stability and suppresses tumorigenesis. *Nature reviews Molecular cell biology* **11**(3)**:** 196-207

Murai J, Huang SY, Renaud A, Zhang Y, Ji J, Takeda S, Morris J, Teicher BA, Doroshow JH, Pommier Y (2013).Stereospecific PARP trapping by BMN 673 and comparison with olaparib and rucaparib.*Mol Cancer Ther*. Dec 19. In press.

Murai J, Huang SY, Das BB, Renaud A, Zhang Y, Doroshow JH, Ji J, Takeda S, Pommier Y (2012).Trapping of PARP1 and PARP2 by Clinical PARP Inhibitors. *Cancer Res* 2(21):5588-5599.

Patel AG, Flatten KS, Schneider PA, Dai NT, McDonald JS, Poirier GG, Kaufmann SH (2012) Enhanced killing of cancer cells by poly(ADP-ribose) polymerase inhibitors and topoisomerase I inhibitors reflects poisoning of both enzymes. *The Journal of biological chemistry* **287**(6)**:** 4198-4210

Sandhu SK, Schelman WR, Wilding G, Moreno V, Baird RD, Miranda S, Hylands L, Riisnaes R, Forster M, Omlin A, Kreischer N, Thway K, Gevensleben H, Sun L, Loughney J, Chatterjee M, Toniatti C, Carpenter CL, Iannone R, Kaye SB, de Bono JS, Wenham RM (2013) The poly(ADP-ribose) polymerase inhibitor niraparib (MK4827) in BRCA mutation carriers and patients with sporadic cancer: a phase 1 dose-escalation trial. *The lancet oncology* **14**(9)**:** 882-892

Scully R, Chen J, Plug A, Xiao Y, Weaver D, Feunteun J, Ashley T, Livingston DM (1997) Association of BRCA1 with Rad51 in mitotic and meiotic cells. *Cell* **88**(2)**:** 265-275

Seruga B, Ocana A, Tannock IF (2011) Drug resistance in metastatic castration-resistant prostate cancer. *Nature reviews Clinical oncology* **8**(1)**:** 12-23

Smith LM, Willmore E, Austin CA, Curtin NJ (2005) The novel poly(ADP-Ribose) polymerase inhibitor, AG14361, sensitizes cells to topoisomerase I poisons by increasing the persistence of DNA strand breaks. *Clinical cancer research : an official journal of the American Association for Cancer Research* **11**(23)**:** 8449-8457

Taylor BS, Schultz N, Hieronymus H, Gopalan A, Xiao Y, Carver BS, Arora VK, Kaushik P, Cerami E, Reva B, Antipin Y, Mitsiades N, Landers T, Dolgalev I, Major JE, Wilson M, Socci ND, Lash AE, Heguy A, Eastham JA, Scher HI, Reuter VE, Scardino PT, Sander C, Sawyers CL, Gerald WL (2010) Integrative genomic profiling of human prostate cancer. *Cancer cell* **18**(1)**:** 11-22

Tutt A, Robson M, Garber JE, Domchek SM, Audeh MW, Weitzel JN, Friedlander M, Arun B, Loman N, Schmutzler RK, Wardley A, Mitchell G, Earl H, Wickens M, Carmichael J (2010) Oral poly(ADP-ribose) polymerase inhibitor olaparib in patients with BRCA1 or BRCA2 mutations and advanced breast cancer: a proof-of-concept trial. *Lancet* **376**(9737)**:** 235-244

Yang Z, Waldman AS, Wyatt MD (2012) Expression and regulation of RAD51 mediate cellular responses to chemotherapeutics. *Biochemical pharmacology* **83**(6)**:** 741-746

Yap TA, Sandhu SK, Carden CP, de Bono JS (2011) Poly(ADP-ribose) polymerase (PARP) inhibitors: Exploiting a synthetic lethal strategy in the clinic. *CA: a cancer journal for clinicians* **61**(1)**:** 31-49

Zhang J, Hu S, Schofield DE, Sorensen PH, Triche TJ (2004) Selective usage of D-Type cyclins by Ewing's tumors and rhabdomyosarcomas. *Cancer research* **64**(17)**:** 6026-6034

Zhang YW, Regairaz M, Seiler JA, Agama KK, Doroshow JH, Pommier Y (2011) Poly(ADP-ribose) polymerase and XPF-ERCC1 participate in distinct pathways for the repair of topoisomerase I-induced DNA damage in mammalian cells. *Nucleic acids research* **39**(9)**:** 3607-3620

Molecular Pharmacology Fast Forward. Published on March 13, 2014 as DOI: 10.1124/mol.113.090688
This article has not been copyedited and formatted. The final version may differ from this version.

FOOTNOTES

Financial Support: This work was supported by the National Institutes of Health Moffitt Cancer Center Support Grant for new faculty recruitment [P30-CA076292-11S5]; and the Conquer Cancer Foundation 2010 Young Investigator Award of American Society of Clinical Oncology [EG ID 1083]

Conflict of interest: No conflict interest in this study.

Molecular Pharmacology Fast Forward. Published on March 13, 2014 as DOI: 10.1124/mol.113.090688
This article has not been copyedited and formatted. The final version may differ from this version.

Legends for Figures

Figure 1. Prostate cancer cells' resistance to drug induced DNA damage and apoptosis under hypoxia is associated with up regulation of Rad51. (A) Growth curves of prostate cancer cells under hypoxic (0.2% oxygen) and normoxic (21% oxygen) culture. The mean and SEM of 3 independent experiments were plotted. (B) Western blots comparing levels of PARP cleavage, Rad51 and γH2AX in untreated control versus 3-day SN38 treatment under normoxia and hypoxia. Increased levels of Rad51 were seen in DU145 and PC3 cells, but not LNCaP cells after SN38 treatment under hypoxia (SNH vs. CH). (C) Percentage of apoptosis as detected by flowcytometry with or without SN38 treatment for 3 days. Each column represents the mean and SEM of 3 independent experiments. White column: 21% oxygen; Black column: 0.2% oxygen; C: untreated control; SN: SN38; CH: untreated under hypoxia; SNH: SN38 treated under hypoxia. β-actin was used as loading control. $*P < 0.05$, $**P < 0.01$, $***P < 0.001$.

Figure 2. Blocking Rad51 up regulation re-sensitizes prostate cancer cells to drug induced DNA damage and apoptosis under hypoxia. (A) Nuclear foci formation of Rad51 and BRCA1 as detected by immunofluorescence in normoxic and hypoxic PC3 cells either untreated (control) or treated with 0.1 μM SN38 for 4 hours. (B) Western blots of DNA ligase IV and DNA-dependent protein kinase (DNA-PK) in untreated control and SN38-treated cells under normoxic and hypoxic conditions. (C) Western blots comparing the Rad51 and γH2AX levels with and without SN38 treatment in untransfected, mock siRNA transfected and RAD51 siRNA transfected PC3 cells under hypoxia. (D) Percentage of apoptosis as detected by flowcytometry in siRNA transfected as well as un-transfected PC3 cells under hypoxia. β-actin was used as loading control.

Molecular Pharmacology Fast Forward. Published on March 13, 2014 as DOI: 10.1124/mol.113.090688
This article has not been copyedited and formatted. The final version may differ from this version.

Three replicates were performed for each experiment. Each column represents the mean and SEM of 3 independent experiments. *$P < 0.05$, **$P < 0.01$, ***$P < 0.001$.

Figure 3. Veliparib enhances the anti-tumor effects of SN38 under hypoxia. (A) Western blots comparing levels of poly(ADP)ribose (PAR) and γH2AX in treated and untreated cells under hypoxia (H): CH, untreated control; SH, SN38; VH, veliparib; V/SH, veliparib plus SN38. **(**B) Neutral comet assay comparing DNA damage/tail moment in treated and untreated cells under hypoxia. The tail moment (*y*-axis) incorporated measurements of both the smallest detectable size of migrating DNA (reflected in the comet tail length) and the number of relaxed/broken pieces (represented by the intensity of DNA in the tail). Each column represent the mean and SEM of tail moments of 50 cells. (C) Percentage of apoptosis as detected by flowcytometry in treated and untreated PC3 cells under hypoxia. (D) Clonogenic assay comparing the effects of hypoxia and 16-hour drug treatment on colony formation of PC3 and DU145 cells. The colony numbers in untreated controls were set as 100%. The colony numbers of each treatment group were divided by those of untreated control and the percentages were reflected in *y*-axes. β-actin was used as loading control. Three replicates were performed for each experiment. Each column represents the mean and SEM of 3 independent experiments. C, untreated control; H, hypoxia; S, SN38; V, veliparib; V/S, veliparib plus SN38. *$P < 0.05$, **$P < 0.01$, ***$P < 0.001$

Figure 4. Veliparib enhances DNA damage and the anti-tumor effects of CPT-11 *in vivo*. (A) Growth curves for PC3 mouse xenografts treated with *schedule A* as described

in results. S: saline control, V: veliparib, C: CPT-11, V+C: the veliparib plus CPT-11 combination. For each treatment group, the growth curve terminated on the day when the first xenograft in the group reached the 1000-mm^3 size. Each tumor volume data point represents mean and SEM of 8 mice. Significant data points were labeled with # in the CPT-11 versus saline comparison and labeled with * in the Valiparib + CPT-11 versus CPT-11 comparison. (B) Growth curves for the PC3 mouse xenografts treated with *schedule B* as described in results. Each tumor volume data point represents mean and SEM of 10 mice. Significant data points were labeled with # in the CPT-11 versus saline comparison and labeled with * in the Valiparib + CPT-11 versus CPT-11 comparison. (C) Survival curve for the PC3 mouse xenografts treated with *schedule B*. Median survival of each treatment group was compared and the log-rank test was used for survival rate analysis. (D) Comparison of IHC positivity and distributions of γH2AX (brown staining, lower panels) and hypoxia/pimonadazole (brown staining, upper panels) among PC3 xenograft sections treated with *schedule B*. (E) Rad51 (brown staining, lower panels) was detected in both pimonadazole positive (brown staining, upper panels) and pimonadazole negative areas on the PC3 xenograft IHC sections treated with *schedule B*.

Figure 5. Transcriptional regulation of Rad51 by E2F1. (A) Quantitative RT-PCR comparing RAD51 mRNA levels in treated and untreated PC3 and DU145 cells under hypoxia (black bars) and normoxia (white bars). The relative abundance of RAD51 mRNA was calculated using GADPH as internal control. (B) Western blots comparing E2F1 and Rad51 levels after 1 day drug treatment under hypoxia. (C) Dual luciferase reporter assay showing enhanced RAD51 promoter activities in PC3 cells after 16 hours

Molecular Pharmacology Fast Forward. Published on March 13, 2014 as DOI: 10.1124/mol.113.090688
This article has not been copyedited and formatted. The final version may differ from this version.

of drug treatment under hypoxia (black bars) and such up-regulated promoter activities were blocked after mutating the E2F1 binding site on the RAD51 promoter (M-SNH vs. SNH and M-V/SH vs. V/SH). Ratios of firefly luciferase versus renilla luciferase activities were shown. (D) E2F1 siRNA decreased E2F1 expression and blocked the increase in RAD51 protein after SN38 treatment under hypoxia (E) Dual luciferase reporter assay comparing RAD51 promoter activities in siRNA transfected or untransfected PC3 cells under different treatments and oxygen. White bars, normoxia; Black bars, hypoxia. (F) ChIP assays showing increased E2F1 occupancy at the RAD51 proximal promoter after SN38 treatment under hypoxia. C, untreated control; SN, SN38, CH, untreated under hypoxia; VH: veliparib treated under hypoxia, SNH: SN38 treated under hypoxia. V/SH: veliparib plus SN38 under hypoxia; M-: mutated E2F consensus binding site on the RAD51 promoter; M-H: untreated cells with mutated E2F consensus binding site on the RAD51 promoter. β-actin was used as loading control. Three replicates were performed for each experiment. Each column represents the mean and SEM of 3 independent experiments. $*P < 0.05$, $**P < 0.01$, $***P < 0.001$.

Figure 6. p53 suppresses Rad51 transcription and sensitizes prostate cancer cells to drug-induced DNA damage. (A) Western blots showing levels of E2F1, Rad51, p53, and p21 at different time points (0, 4, 8, 12 and 24h) after SN38 treatment in LNCaP cells under hypoxia. (B) Western blots showing restoration of wild type p53 in PC3 cells after infection with p53/GFP adenovirus 5 (ad-p53). Levels of rH2Ax and Rad51 in PC3 cell with or without SN38 treatment under hypoxia were compared among uninfected, GFP adenovirus 5 vector (V) and p53/GFP adenovirus 5 (ad-p53) infected cells. (C) Dual

luciferase reporter assays of RAD51 promoter activities in LNCaP with or without SN38 treatment for 16h under hypoxia. (D) Chip assays comparing RAD51 promoter occupancy by E2F1 and p53 with or without SN38 treatment under hypoxia. C, untreated control; SN, SN38, CH, untreated under hypoxia; SNH: SN38 treated under hypoxia. Tubulin was used as loading control. Three replicates were performed for each experiment. Each column represents the mean and SEM of 3 independent experiments. $*P < 0.05$, $**P < 0.01$, $***P < 0.001$.

Figure 7. Schematic diagram of prostate cancer cells' response to drug induced double strand DNA breaks under hypoxia. Down regulation of RAD51 promoter by p53 undermines homologous recombination repair and lead to cell death in cells with wild type p53 under hypoxia. Up regulation of RAD51 promoter by E2F1 in p53 mutant cells facilitate DNA repair and drug resistance. Such resistance can be overcame by adding PAPR inhibitor (PARPi), which trapped PARP at DNA breaks and blocks access of DNA repair proteins like Rad51. PAPRi by itself was not sufficient to cause detrimental DNA double strand breaks to prostate cancer cells under hypoxia.

Molecular Pharmacology Fast Forward. Published on March 13, 2014 as DOI: 10.1124/mol.113.090688
This article has not been copyedited and formatted. The final version may differ from this version.

Figure 1

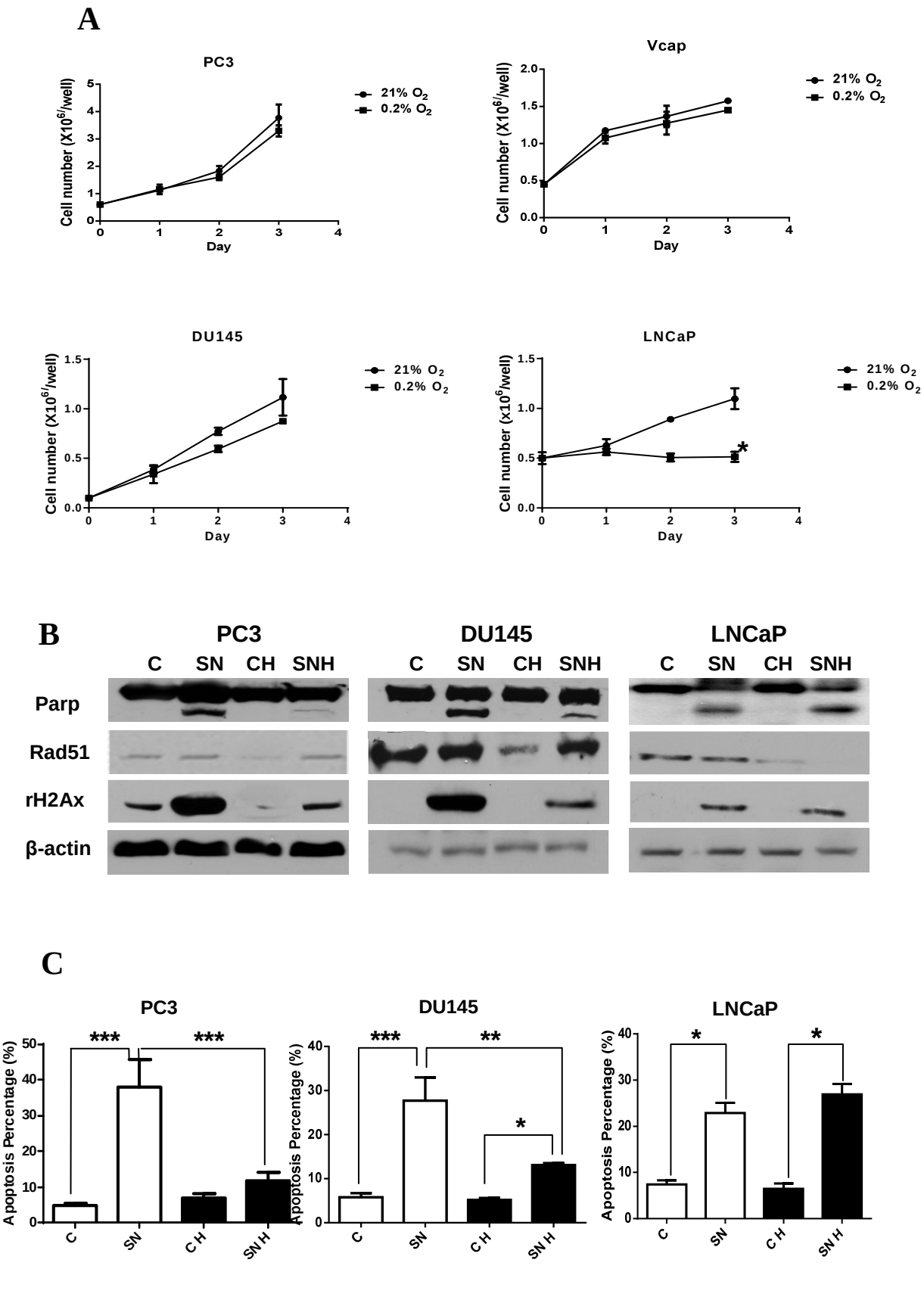

Molecular Pharmacology Fast Forward. Published on March 13, 2014 as DOI: 10.1124/mol.113.090688
This article has not been copyedited and formatted. The final version may differ from this version.

Figure 2

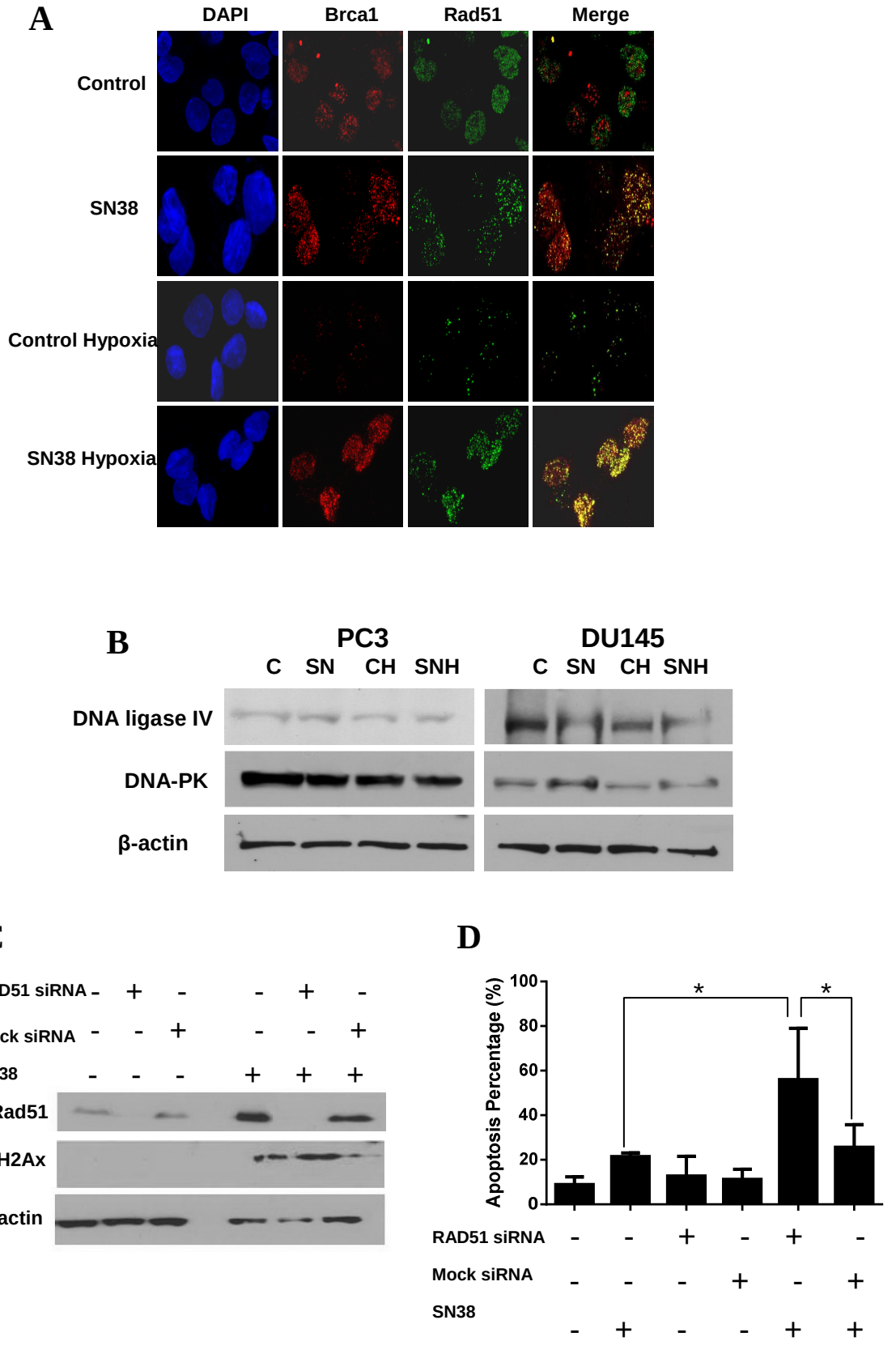

Molecular Pharmacology Fast Forward. Published on March 13, 2014 as DOI: 10.1124/mol.113.090688
This article has not been copyedited and formatted. The final version may differ from this version.

Figure 3

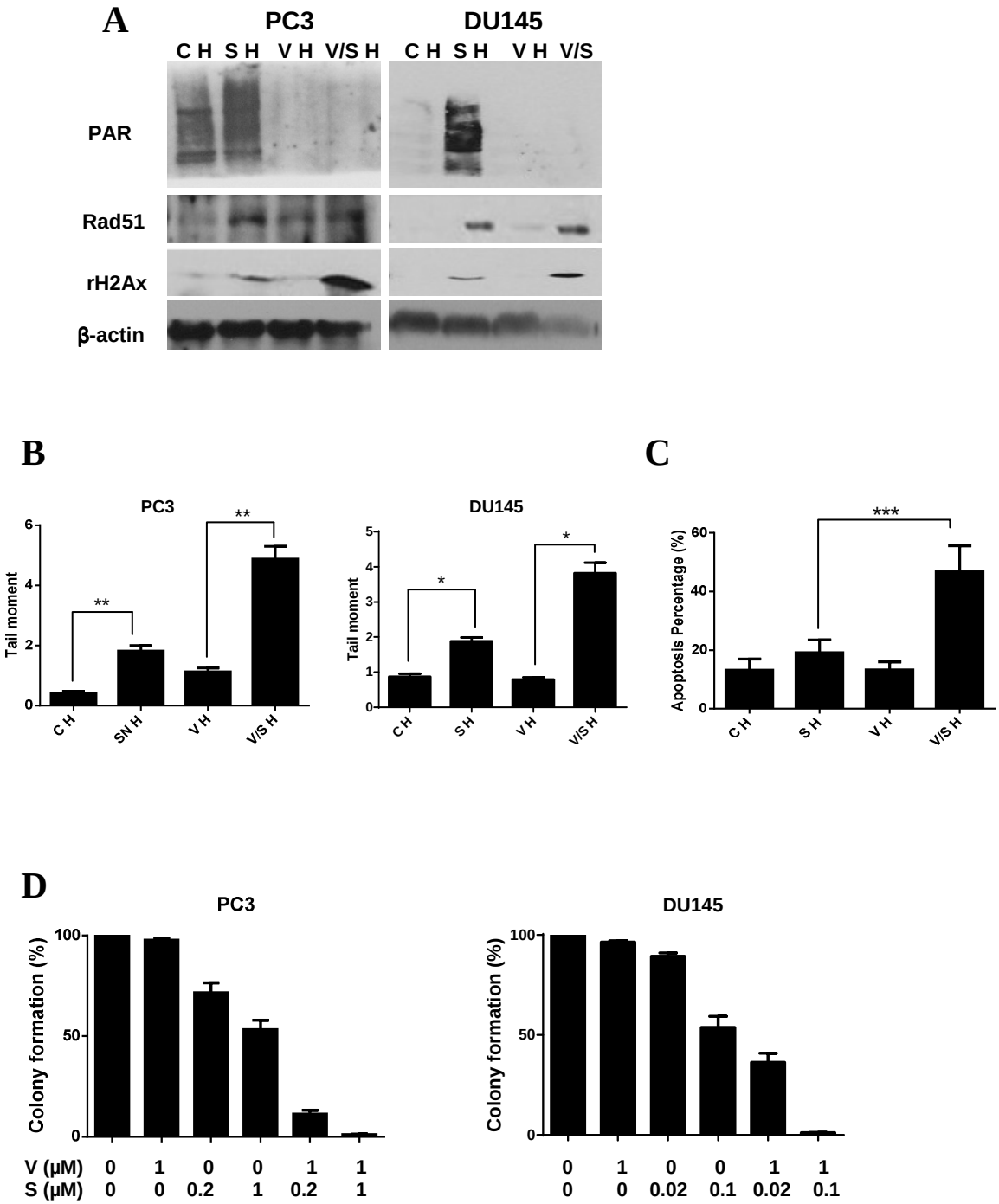

Molecular Pharmacology Fast Forward. Published on March 13, 2014 as DOI: 10.1124/mol.113.090688
This article has not been copyedited and formatted. The final version may differ from this version.

Figure 4

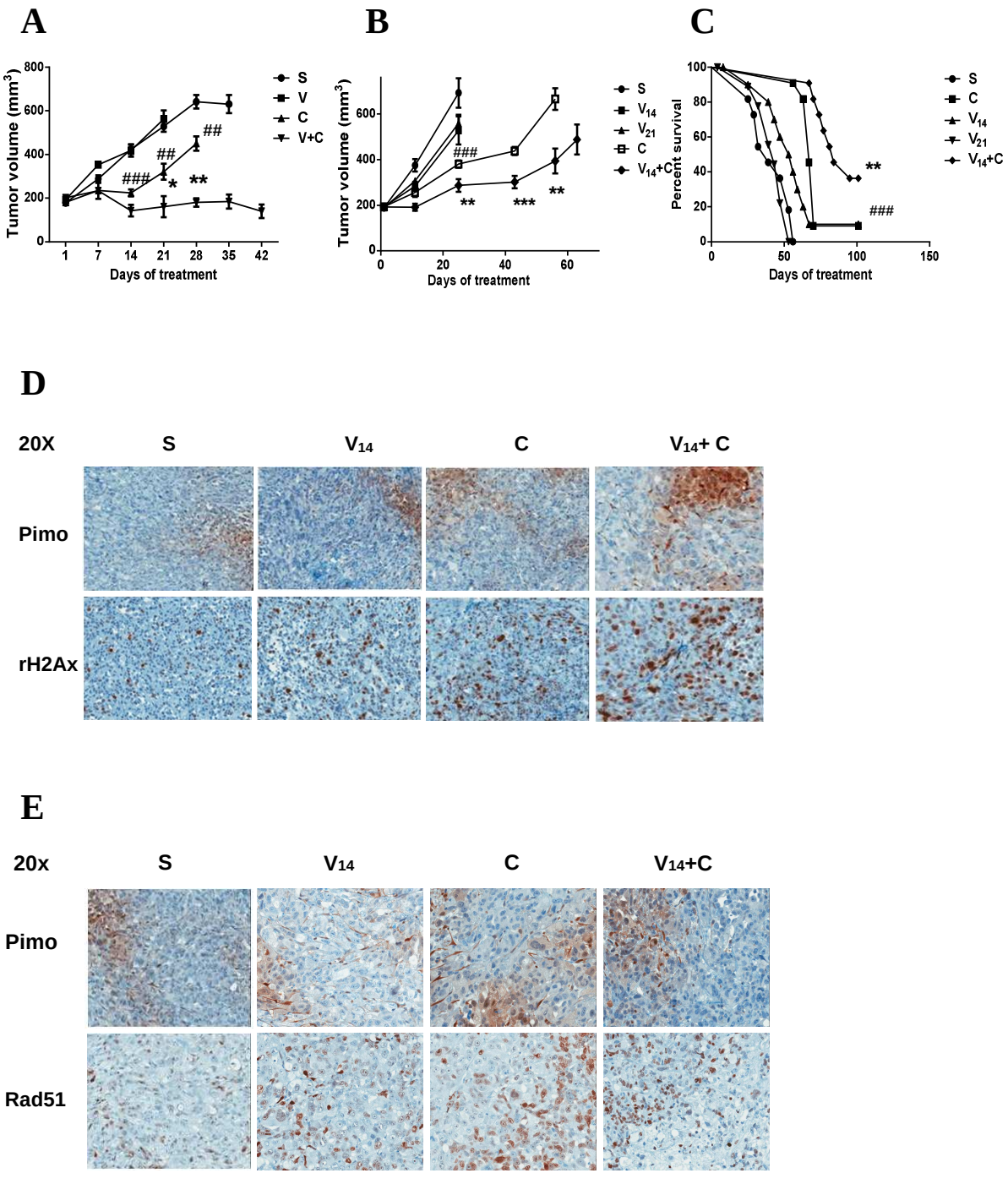

Molecular Pharmacology Fast Forward. Published on March 13, 2014 as DOI: 10.1124/mol.113.090688
This article has not been copyedited and formatted. The final version may differ from this version.

Figure 5

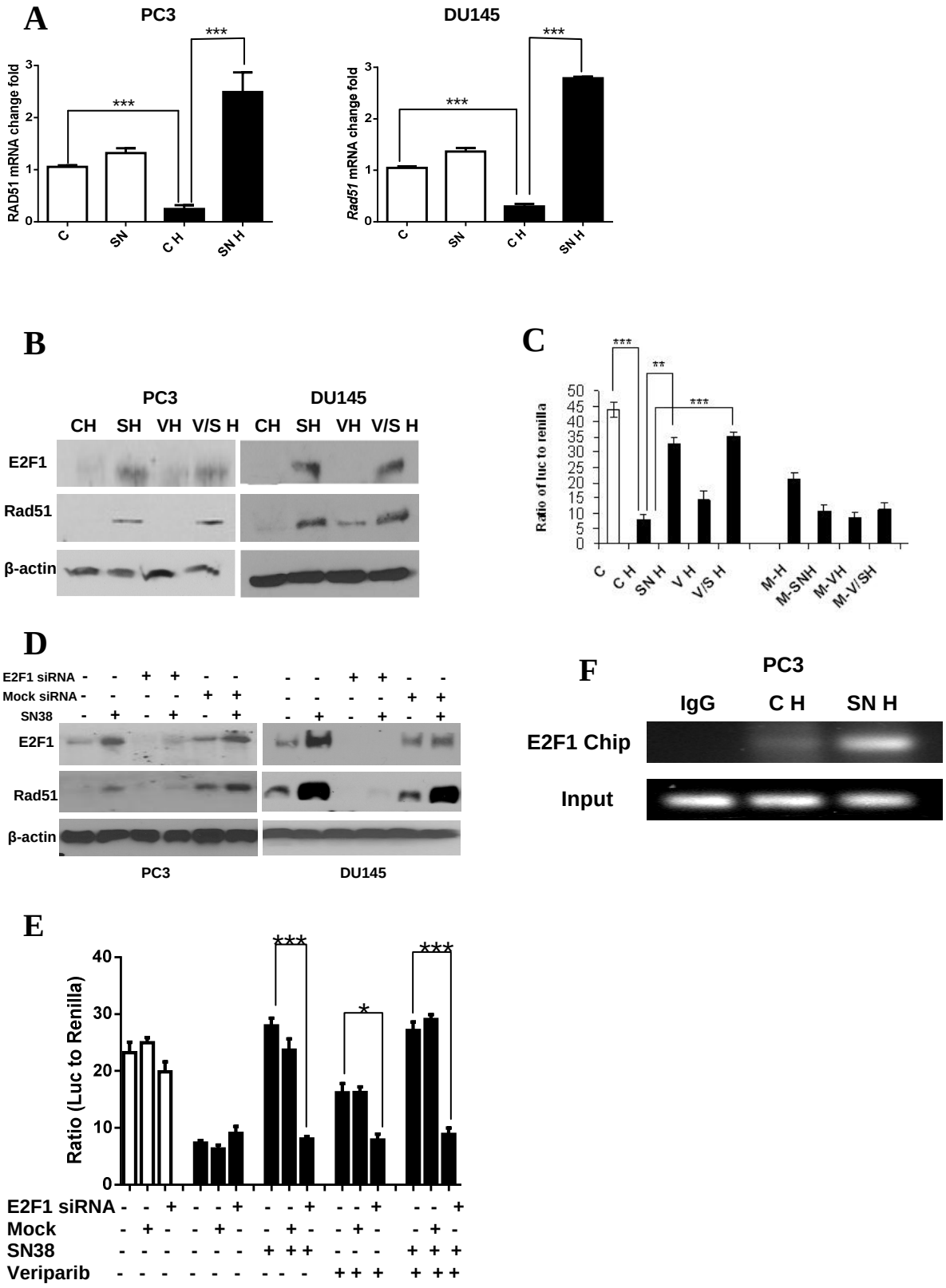

Molecular Pharmacology Fast Forward. Published on March 13, 2014 as DOI: 10.1124/mol.113.090688
This article has not been copyedited and formatted. The final version may differ from this version.

Figure 6

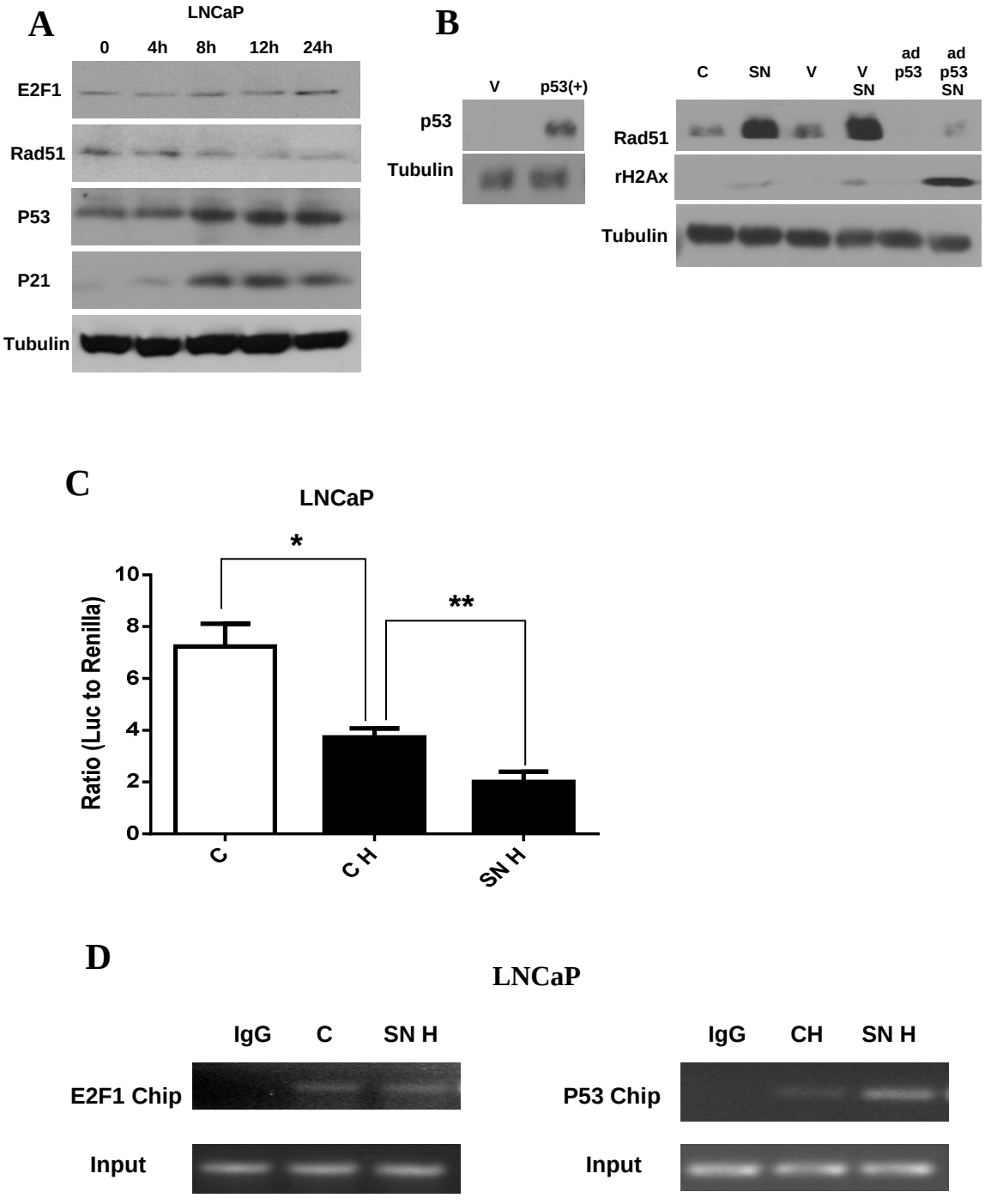

Molecular Pharmacology Fast Forward. Published on March 13, 2014 as DOI: 10.1124/mol.113.090688
This article has not been copyedited and formatted. The final version may differ from this version.

Figure 7